

Photohydration of Benzophenone in Aqueous Acid[†]

Markus Ramseier, Paul Senn, and Jakob Wirz*

Departement Chemie der Universität Basel, Klingelbergstrasse 80, CH-4056 Basel, Switzerland

Received: August 1, 2002; In Final Form: November 13, 2002

Why is the triplet state of aromatic ketones quenched by protons? The long-known but unexplained quenching process was investigated in detail for benzophenone (**1**). Adiabatic protonation of triplet benzophenone, ³**1**, encounters a state symmetry-imposed barrier, because the electronic structure of ³**1** is n,π^* , while that of its conjugate acid, ³**1**H⁺, is π,π^* . Hence, the rate of protonation of ³**1**, $k_{H^+} = 6.8 \times 10^8 \text{ M}^{-1} \text{ s}^{-1}$, is well below the diffusion-controlled limit. The short-lived transient intermediate formed by protonation of ³**1** in 0.1–1 M aqueous HClO₄ ($\lambda_{\text{max}} = 320$ and 500 nm, $\tau = 50$ ns) is not ³**1**H⁺, as was assumed in previous studies. The latter ($\lambda_{\text{max}} = 385$ nm) is detectable only in acidified acetonitrile or in highly concentrated aqueous acid (>5 M HClO₄), where water activity is low. In moderately concentrated aqueous acids, adiabatic protonation of ³**1** is the rate-limiting step preceding rapid adiabatic hydration of a phenyl ring, ³**1**H⁺ + H₂O → ³**1**·H₂O, $k_0 = 1.5 \times 10^9 \text{ s}^{-1}$. These findings lead to a revised value for the acidity constant of protonated ³**1**, $\text{p}K_{\text{a}}(^3\text{1H}^+) = -0.4 \pm 0.1$. Acetophenone (**2**) and several derivatives of **1** and **2** undergo a similar reaction sequence in aqueous acid. The acid-catalyzed photohydration of parent **1** and **2** is reversible. In meta-fluorinated derivatives, the reaction results in a clean and efficient formation of the corresponding phenols, a novel aromatic photosubstitution reaction. This indicates that hydration of ³**1**H⁺ occurs predominantly at the meta position. A long-lived transient ($\lambda_{\text{max}} = 315$ nm, $\tau = 5.4$ s) left after the decay of ³**1**·H₂O is attributed to a small amount of *ortho*-**1**·H₂O that regenerates **1** more slowly.

Introduction

Since Hammond and co-workers¹ elucidated the mechanism of the photoreduction of benzophenone (**1**) in 1962, the photophysical and photochemical properties of this molecule are known to any photochemist. Equally well-established is the fact that phenols become stronger acids upon electronic excitation,² while aromatic ketones become stronger bases. Thirty years ago, Ledger and Porter³ reported that the phosphorescence of **1** in aqueous solution is quenched by protons with a rate constant of $6 \times 10^8 \text{ M}^{-1} \text{ s}^{-1}$. They noted that “the quenching action of the proton is not understood”. Several studies have since dealt with the photoprocesses of **1** in aqueous solution.^{4–13} Wyatt and co-workers^{4,5} investigated the initial absorbances and lifetimes of the triplet intermediates formed by flash photolysis of **1** over a wide range of acid concentrations and determined a $\text{p}K_{\text{a}}$ of 1.5 ± 0.1 for the adiabatic dissociation constant of protonated triplet **1**, ³**1**H⁺. They found that the lifetime of ³**1** drops below 100 ns around $\text{pH} \approx 0$, whereas that of its conjugate acid ³**1**H⁺ rises to 50 μs in degassed solutions of still higher acidities, and they concluded, “A possible explanation is that water is an effective quencher of [³**1**H⁺].” Despite a number of follow-up studies,^{6–8} a satisfactory explanation for this puzzling phenomenon has not come forth.

We report an investigation of **1** and of acetophenone (**2**) in aqueous acid by picosecond pump–probe spectroscopy, nanosecond laser flash photolysis (LFP), conventional flash photolysis, and photoacoustic calorimetry. We conclude that acid-catalyzed photohydration is responsible for the triplet quenching process observed in moderately acidic aqueous solutions.

Photohydration of the parent ketones **1** and **2** is reversible. However, in *m*-fluoro derivatives of **1** and **2**, it results in efficient formation of the corresponding *m*-hydroxy ketones.

Experimental Section

The instruments used for picosecond pump–probe spectroscopy and for nanosecond LFP have been described previously.¹⁴ Briefly, pump–probe experiments were carried out using a 248 nm excitation pulse and a continuum probe pulse (300–700 nm), both with subpicosecond lifetimes. The delay line spanned a time range of 1.8 ns. Acetonitrile (2.0 M, about 10 vol %) was added as a cosolvent to achieve the required absorbance by **1** ($A = 1$ at the excitation wavelength of 248 nm, path length 2 mm) in neutral aqueous solutions. Addition of acetonitrile was not required to increase the solubility of **1** in aqueous acid. Nanosecond laser pulses at 248 or 351 nm were obtained from a Lambda Physik Compex 205 excimer laser (pulse width ca. 15 ns, pulse energy 100–600 mJ). Pulses at 308 nm were taken from a Lambda Physik EMG 101 MSC excimer laser (pulse width ca. 20 ns, pulse energy 50–100 mJ). Kinetic (1P28 photomultiplier) and spectrographic detection (MCP-gated diode array) of the transient absorption were available. Most kinetic measurements were done at ambient temperature (22 ± 2 °C). Perchloric acid solutions were made up by weighing the appropriate amounts of 70% (by weight) ultrapure HClO₄ and dilution with doubly distilled water.

Fluorescence spectra were recorded on a Spex Fluorolog 111 instrument equipped with an R928 photomultiplier. Excitation spectra were corrected with a built-in Rhodamine-6G quantum counter. Fluorescence lifetimes were measured by excitation with subpicosecond pulses from a Ti:Sapphire laser (Clark MXR CPA-2001; frequency-doubled, 388 nm; frequency-doubled NOPA output, 270 nm). The emission spectra were recorded

* To whom correspondence should be addressed. Tel. +41 61 267 38 42. Fax: +41 61 267 38 55. E-mail: J.Wirz@unibas.ch.

[†] Part of the special issue “George S. Hammond & Michael Kasha Festschrift”.

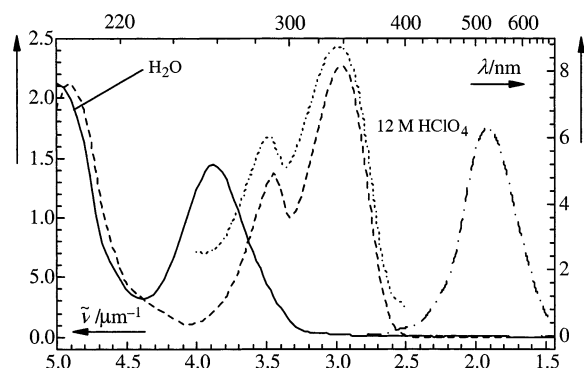


Figure 1. Absorption spectra of **1** (ca. 4×10^{-5} M) in neutral (—) and 12 M HClO₄ (---) aqueous solution (left-hand scale). Fluorescence emission (— · —, excitation wavelength 335 nm) and excitation (···, emission monitored at 522 nm) spectra of **1** in 12 M aqueous HClO₄ (right-hand scale).

with a streak camera (Hamamatsu C5680) operated at 50 ps time resolution.

The setup used for photoacoustic calorimetry has been described in detail.¹⁵ The design of the front-face irradiation flow cell and the algorithm used for the analysis of the sound waves recorded by the microphone were those of Caldwell, Melton, and co-workers.¹⁶ Solutions of 2-hydroxybenzophenone were used as a reference. The photoacoustic waveforms of the sample (*E* wave) were analyzed by convoluting the reference signal (*T* wave) with a dual or triple exponential heat deposition function and least-squares fitting of the resulting waveforms to the observed *E* wave. Five independent waveforms from separate experiments were analyzed for a given set of conditions. Goodness-of-fit was judged by comparing the residuals with the minimal error expected to arise from the eight bit resolution of the transient digitizer.

Photohydrolysis of 3,4-Difluoroacetophenone. A solution of 3,4-difluoroacetophenone (44 mg) in 1 M aqueous HClO₄ (300 mL with 25% acetonitrile) was irradiated at 254 nm (low-pressure mercury arc) until the product absorption at 298 nm reached a maximum. The mixture was extracted with *tert*-butylmethyl ether, dried with MgSO₄, and evaporated, leaving a yellow oil that was chromatographed on silica using petroleum ether and methyl acetate (4:1) as an eluent. Besides 8 mg of the starting material, 16 mg of 4-fluoro-3-hydroxyacetophenone was isolated; mp 113–115 °C. ¹H NMR (CDCl₃, TMS): δ = 2.58 (s, 3H, Me), 5.74 (broad s, 1H, OH), 7.14 (dd, 1H, H₅, *J* = 8.2 and 8.7 Hz), 7.51 (m, 1H, H₆), 7.64 ppm (dd, 1H, H₂, *J* = 8.4 and 2.1 Hz). ¹³C NMR (CDCl₃, TMS): δ = 154.22 (d, C₄, *J* = 247 Hz), 143.84 (d, C₃, *J* = 14.7 Hz), 134.33 (d, C₁, *J* = 0.8 Hz), 121.75 (d, C₆, *J* = 7.6 Hz), 117.65 (d, C₂, *J* = 3.3 Hz), 115.73 (d, C₅, *J* = 19.0 Hz), 196.76 (s, C₇), 26.53 ppm (s, C₈). MS (*M*⁺): *m/e* 154. UV ($\lambda_{\text{max}}/\text{nm}$ [$\log(\epsilon/\text{M}^{-1} \text{cm}^{-1})$): in 0.1 M aqueous HClO₄: 253 [3.89], 298 [3.39]; in 0.1 M NaOH: 236 [4.34], 264 sh [3.7], 336 [3.43].

Quantum Yields of Photosubstitution. Fluorinated derivatives of **1** and **2** were irradiated at 254 nm with a medium pressure mercury arc (Hanau St 41, interference band pass filter) in degassed, 0.1 M aqueous HClO₄. The reaction progress was monitored by UV spectrophotometry. Quantum yields were determined using azobenzene in methanol as an actinometer.¹⁷

Results

Absorption and Fluorescence Emission. Figure 1 displays the absorption spectra of **1** in neutral water and in 12 M aqueous HClO₄. The latter is attributed to oxygen-protonated benzophe-

none, **1H**⁺.⁴ Also shown are the fluorescence excitation and emission spectra of **1** in 12 M aqueous HClO₄ solution. The fluorescence of **1** in neutral aqueous solution was below the detection limit of the conventional fluorescence spectrometer used. Weak emission of **1H**⁺ ($\lambda_{\text{max}} = 522$ nm) was observed in solutions with acid concentrations exceeding 1 M. Ground state protonation of **1** is negligible in 5.8 M HClO₄ ($H_0 = -2.7$),¹⁸ and the excitation spectrum of the fluorescence by **1H**⁺ in 5.8 M HClO₄ matched the absorption spectrum of neutral **1**. Thus, adiabatic protonation of **1** occurs with low efficiency in the excited singlet state. The fluorescence lifetimes of **1H**⁺ in 5.8 M (excitation at 270 nm) and 12 M air-saturated aqueous HClO₄ solution (excitation at 388 nm) were equal within experimental error, $\tau = 700 \pm 30$ ps.

Pump–Probe Spectroscopy. Transient absorption spectra obtained with **1** in neutral aqueous solution are shown in Figure 2. The spectra taken during the initial period (0–5 ps delay,¹⁹ not shown) were distorted by two photon absorption and exhibited spectral broadening arising from vibrational relaxation. The first spectrum shown (6 ps delay) is attributed to the lowest excited singlet state of **1** ($\lambda_{\text{max}} = 335$ and ca. 575 nm)²⁰ as well as some broad absorption arising from solvated electrons ($\lambda_{\text{max}} = 720$ nm). Solvated electrons are also formed in the absence of a solute due to multiphoton absorption of the laser pulse by water.

The initial changes in the transient spectra are attributed²⁰ to intersystem crossing (ISC) from the lowest excited singlet state, ¹**1**, to the lowest triplet state, ³**1**. Factor analysis²¹ of the spectra observed in the region of 500–550 nm required two significant components only, and global fitting to a single exponential rate law gave a singlet lifetime of 6.4 ± 0.2 ps. The spectrum of ³**1** ($\lambda_{\text{max}} = 330$ and 525 nm) persisted up to the maximum delay of 1.8 ns.

Pump–probe spectra obtained with **1** in 1 M aqueous HClO₄ are shown in Figure 3. The spectral changes that are observed during the first 30 ps are quite similar to those in neutral water (Figure 2). However, two additional processes are indicated by the subsequent spectral changes. Factor analysis using the wavelength range of 450–550 nm indicated that four components are required for an adequate description of the spectral matrix and that a triexponential function is needed to fit the kinetics. A global least-squares fit of a triexponential function is shown in Figure 4. The spectral changes and the rate constant associated with the first process, $k_1 = (1.35 \pm 0.09) \times 10^{11} \text{ s}^{-1}$, are the same as in neutral water (Figure 2) and are attributed to ISC of **1**. The decay of the broad absorption arising from solvated electrons ($\lambda_{\text{max}} = 720$ nm) due to trapping by H⁺ provides the second rate constant, $k = (1.7 \pm 0.2) \times 10^{10} \text{ s}^{-1}$. A bimolecular rate constant $k = 2.3 \times 10^{10} \text{ M}^{-1} \text{ s}^{-1}$ is commonly quoted for this process,²² but that value pertains to low ionic strengths. The rate constant reported for the capture of solvated electrons by protons in 1 M aqueous HClO₄ is $k = 1.1 \times 10^{10} \text{ s}^{-1}$.²³

The final process is hard to discern by visual inspection of Figure 3. Proper analysis reveals that the band shapes and maxima gradually change from those of ³**1** ($\lambda_{\text{max}} = 330$ and 525 nm) to those of a species with $\lambda_{\text{max}} = 320$ and 500 nm, which is attributed to the triplet state of a hydrate of **1**, ³**1**·H₂O.²⁰ The process is not complete within 2 ns after excitation (cf. Figure 4), and the associated rate constant is not well-defined in this time window. To avoid the perturbing influence arising from the decay of the solvated electrons, global analysis of four series of measurements in 1 M HClO₄ was restricted to the time window of 0.2–1.8 ns. In this way, an average value of $k_3 =$

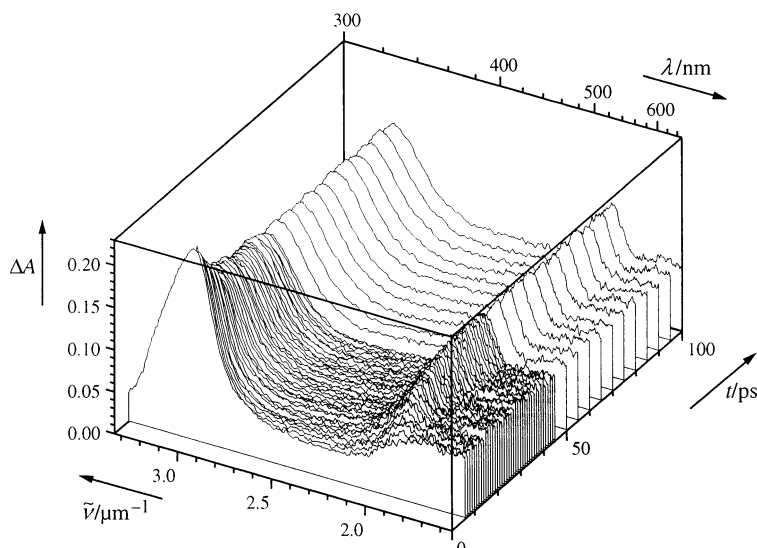


Figure 2. Pump-probe transient absorption spectra of **1** (5×10^{-4} M) in neutral water detected with delays of 6–100 ps¹⁹ relative to the excitation pulses (248 nm, 0.5 ps half-width, 1 mJ per pulse).

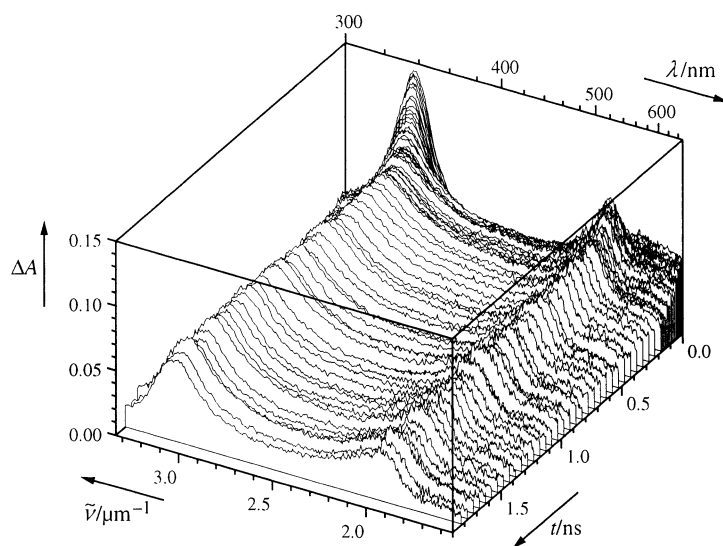


Figure 3. Pump-probe transient absorption spectra of **1** (8×10^{-4} M) in 1 M aqueous HClO₄ detected with delays of 5–1826 ps¹⁹ relative to the excitation pulses (248 nm, 0.5 ps half-width, 1 mJ per pulse).

$(5 \pm 1) \times 10^8$ s⁻¹ was obtained for the rate constant of the slow process.

Substantially different spectral changes were observed by pump-probe spectroscopy of **1** in 4 M HClO₄ (not shown). The initial changes with a rate constant of about $k_1 = 2 \times 10^{11}$ s⁻¹ are again attributed to ISC of **1** to **³1**. The kinetics of this process was somewhat distorted by the nearly simultaneous reaction of the solvated electrons with protons, for which a rate constant of about 5×10^{11} s⁻¹ is expected in this medium. Following these processes, a new, broad band with $\lambda_{\max} = 385$ nm is formed. At the same time, the absorption band at 525 nm, due to **³1**, shifts to 500 nm and is reduced in intensity. The rate constant of this process, determined from a biexponential fit to the series of spectra in the range of 360–430 nm, where interference by the absorption of solvated electrons is negligible, is $k_2 \approx 3 \times 10^{10}$ s⁻¹. The species formed here is assigned to the triplet state of carbonyl-protonated benzophenone, **³1H⁺**.²⁰ At delay times >175 ps, the 385 nm absorption band due to **³1H⁺** decays almost completely, leaving a similar end spectrum as in Figure 3. The rate constant of the last reaction is $k_3 \approx 1.2 \times 10^9$ s⁻¹.

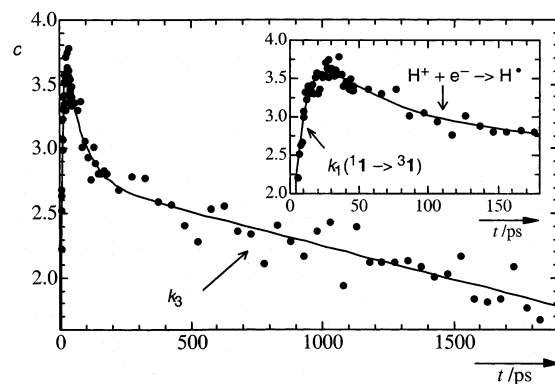


Figure 4. Loading coefficients c (•) of the first eigenvalue determined by factor analysis of the spectral matrix (450–550 nm) that is shown in Figure 3. The solid line shows the result of a global nonlinear least-squares fit of a triexponential function. The corresponding fit parameters (first-order rate constants) are given in the text. The inset is an expanded view of the first 180 ps.

Pump-probe spectra determined with 5.8 M HClO₄ solutions of **1** are shown in Figure 5. Again, ISC of **1** to **³1** with the

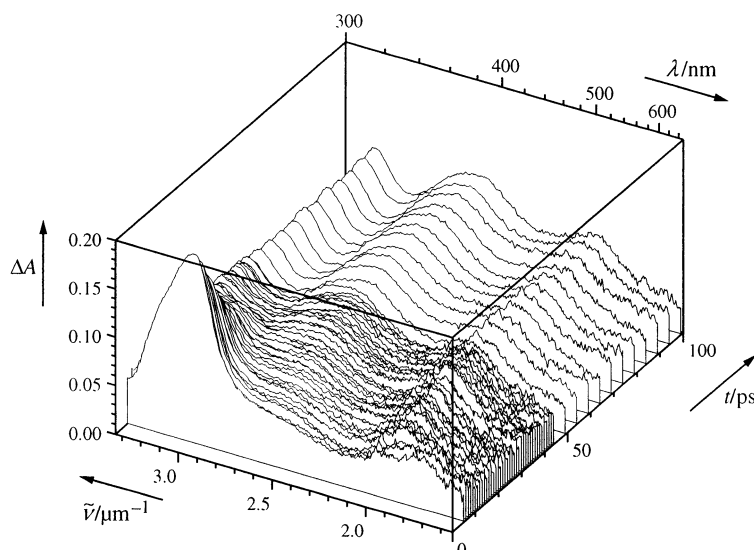


Figure 5. Pump–probe transient absorption spectra of **1** (7×10^{-4} M) in 5.8 M aqueous HClO₄ detected with delays of 5–100 ps¹⁹ relative to the excitation pulses (248 nm, 0.5 ps half-width, 1 mJ per pulse).

TABLE 1: Observed First-Order Rate Constants k_1 – k_5 in Air-Saturated Aqueous HClO₄ (Room Temperature, 22 ± 2 °C)^a

[H ⁺] (M)	pH or H_0 ^b	k_1 (10^{11} s ⁻¹ c)	k_2 (10^{10} s ⁻¹ c)	k_3 (10^8 s ⁻¹ c)	k_4 (10^7 s ⁻¹ c)	k_5 (s ⁻¹ c)
0	neutral	1.61 ± 0.05 (2)		$(7.3 \pm 0.1) \times 10^{-3}$ (8)		
0.001	3.0			$(1.16 \pm 0.02) \times 10^{-2}$ (7)		
0.005	2.3			$(2.71 \pm 0.06) \times 10^{-2}$ (3)		0.154
0.008	2.1			$(3.65 \pm 0.02) \times 10^{-2}$ (5)		
0.01	2.0			$(4.57 \pm 0.04) \times 10^{-2}$ (8)		
0.02	1.7			$(9 \pm 1) \times 10^{-2}$ (2)		
0.03	1.5			$(1.13 \pm 0.05) \times 10^{-1}$ (3)		
0.05	1.3			$(1.28 \pm 0.04) \times 10^{-1}$ (7)		
0.10	0.97			$(2.2 \pm 0.3) \times 10^{-1}$ (4)		0.156 ± 0.003 (4)
0.20	0.65				2.2 ± 0.1 (4)	
0.50	0.18				2.0 ± 0.1 (6)	
1.0	-0.25	1.2 ± 0.2 (2)		5 ± 1 (4)	1.9 ± 0.1 (6)	0.360 ± 0.002 (3)
1.5	-0.56			9 ± 2 (2)		
2.0	-0.82	1.6 ± 0.2 (3)	1.0 ± 0.1 (3)	11 ± 2 (3)		0.399 ± 0.003 (4)
2.5	-1.1	1.4 ± 0.3 (1)		12 ± 1 (1)		
3.0	-1.3	1.7 ± 0.2 (3)	1.3 ± 0.2 (3)	10.9 ± 0.7 (3)	2.2 ± 0.1 (6)	0.53 ± 0.01 (4)
4.0	-1.7	1.8 ± 0.9 (2)	3.0 ± 0.2 (2)	12 ± 2 (2)	2.4 ± 0.1 (6)	1.42 ± 0.01 (4)
5.0	-2.22					2.88 ± 0.08 (5)

^a Solutions used for pump–probe measurements contained 10% acetonitrile. ^b Values of the H_0 acidity function (ref 18) are given for [H⁺] \geq 0.1 M. ^c Number of measurements given in brackets.

associated spectral changes ($\lambda_{\max} = 335$ and 575 nm shifting to 330 and 525 nm) is the first process, $k_1 \approx 8 \times 10^{10}$ s⁻¹. Almost as fast, $k_2 \approx 5 \times 10^{10}$ s⁻¹, is the formation of a broad absorption band with $\lambda_{\max} = 385$ nm, which is attributed to adiabatic protonation of ³**1** at the carbonyl oxygen yielding ³**1**H⁺. Further small changes, which cannot be assigned, occurred at longer delays.

Nanosecond Flash Photolysis (LFP). The transient absorption spectrum of triplet benzophenone (³**1**) obtained by 248 nm excitation of **1** (4×10^{-5} M) in neutral water ($\lambda_{\max} = 330$ and 525 nm, not shown) was in excellent agreement with that obtained at the maximum delay (1.8 ns) in the pump–probe experiment (Figure 2). The decay of ³**1** was dominated by oxygen quenching and obeyed the first-order rate law accurately. An average rate constant $k_3 = (7.3 \pm 0.1) \times 10^5$ s⁻¹ (air-saturated solutions) was obtained from eight measurements at different wavelengths in the range of 315–600 nm. The decay rate of ³**1** increased linearly with increasing acid concentration (k_3 , Table 1).

Transient spectra obtained by LFP of **1** (4×10^{-5} M) in 1.0 M HClO₄ are shown in Figure 6, together with two of the traces obtained by pump–probe spectroscopy. The transient spectrum

obtained immediately after the nanosecond laser pulse (marked “10 ns”) is attributed to the triplet state of the hydration product, ³**1**·H₂O.²⁰ Comparison with the pump–probe spectra recorded with delays of 176 and 1826 ps in the same medium indicates that the conversion of ³**1** to ³**1**·H₂O is not complete within 1826 ps (cf. Figures 3 and 4). Kinetic measurements by nanosecond LFP at various wavelengths from 315 to 520 nm gave an average rate constant of $k_4 = (1.9 \pm 0.1) \times 10^7$ s⁻¹ for the decay of ³**1**·H₂O. The same initial transient spectra and decay rate constants were observed by LFP of aqueous solutions containing from 0.20 to 4.0 M HClO₄ (Table 1). The temperature dependence of the rate constant k_4 was measured with 1 M HClO₄ solutions ($T = 274$ – 335 K, 22 measurements). An Arrhenius plot of these data was linear and gave the activation parameters $A = (1.6 \pm 0.4) \times 10^8$ s⁻¹ and $E_a = 1.13 \pm 0.10$ kcal mol⁻¹.

The transient spectrum generated by LFP of **1** in 5.8 M HClO₄ is substantially different (Figure 7). The initial spectrum agrees well with that observed at maximum delay by pump–probe spectroscopy with the same solvent (Figure 5). It also agrees closely with the initial transient spectrum recorded by LFP of **1** in a 0.5 M solution of HClO₄ (70%) in acetonitrile (not shown)

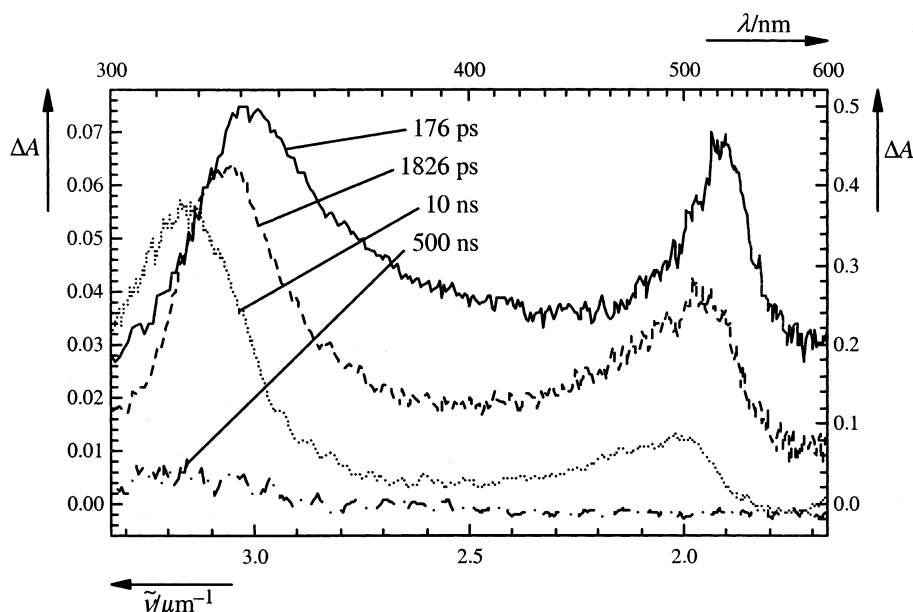


Figure 6. Transient absorption spectra obtained with **1** in 1 M HClO₄. The two upper traces (left-hand absorbance scale) were obtained by pump-probe spectroscopy, and the two lower ones (right-hand absorbance scale) were obtained by LFP. Delay times relative to the excitation flash at 248 nm are shown.

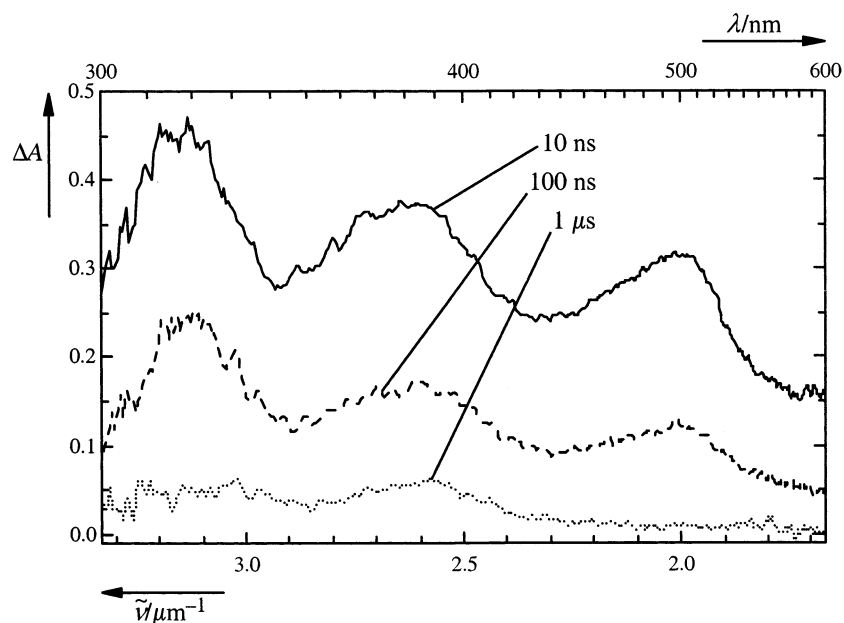


Figure 7. LFP of **1** (4.9×10^{-5} M) in 5.8 M aqueous HClO₄. Delay times relative to the excitation pulse at 248 nm (15 ns, 150 mJ) are shown.

and is attributed to protonated triplet benzophenone, ${}^3\mathbf{1H}^+$. It decays with a first-order rate constant of $(8.7 \pm 0.4) \times 10^6 \text{ s}^{-1}$. Similar results were obtained with 6.0 M HClO₄. In this medium, the transient decays with a rate constant of $(5.6 \pm 0.1) \times 10^6 \text{ s}^{-1}$.

LFP of **1** in 12 M HClO₄, where it is protonated in the ground state (Figure 1), gave weak, broad transient absorption with maxima at about 390 and 500 nm, which is attributed to ${}^3\mathbf{1H}^+$. In this medium, bleaching of the ground state absorption of $\mathbf{1H}^+$ hides the 320 nm band of ${}^3\mathbf{1H}^+$ (Figures 5 and 7). Transient ${}^3\mathbf{1H}^+$ decays with a first-order rate constant of $(1.6 \pm 0.1) \times 10^5 \text{ s}^{-1}$ in air-saturated, 12 M HClO₄.

Conventional (ms) Flash Photolysis. Excitation of **1** in aqueous acid with a discharge flash lamp (up to 1000 J electrical energy, 30 μs half-width) produced a long-lived transient absorbing below 350 nm, $\lambda_{\text{max}} = 315 \text{ nm}$, which is attributed to $\mathbf{1}\cdot\text{H}_2\text{O}$.²⁰ The same absorption was left after the

decay of the transient ${}^3\mathbf{1}\cdot\text{H}_2\text{O}$ in the spectra determined by nanosecond LFP (Figure 6, 500 ns delay). A dilution experiment ($[\mathbf{1}] = 1\text{--}20 \times 10^{-6} \text{ M}$) in 0.1 M HClO₄ proved that the amount of $\mathbf{1}\cdot\text{H}_2\text{O}$ was linearly related to the amount of light absorbed, i.e., that the yield of $\mathbf{1}\cdot\text{H}_2\text{O}$ did not depend on the concentration of **1**. The lifetime of $\mathbf{1}\cdot\text{H}_2\text{O}$ was $\tau = 5.4 \pm 1.0 \text{ s}$ in 0.1 M aqueous HClO₄. Formation of this transient requires both water and acid. No such transient was formed in solutions of **1** in acetonitrile that was acidified with HCl gas or concentrated HClO₄.

The yield of $\mathbf{1}\cdot\text{H}_2\text{O}$ increased with acid concentration in dilute, air-saturated aqueous HClO₄ (0.001–0.10 M). The inverse of the initial absorbance A_0 at 310 nm was linearly related to the inverse of $[\text{H}^+]$. Linear regression (eight data points) gave an intercept of 30.0 ± 0.1 and a slope of $(5.86 \pm 0.03) \times 10^{-2} \text{ M}$. Upon further increase of the acid concentration, A_0 reached a maximum value at about 1 M HClO₄ and decreased

TABLE 2: Results of B3LYP/6-31G* Calculations

compd	<i>E</i> (hartree)	ZPE (hartree)	<i>H</i> (298 K) ^a (hartree)	<i>S</i> ^o (298 K) (cal K ⁻¹ mol ⁻¹)	ΔH° (298 K) (kcal mol ⁻¹)
<i>o</i> -1•H ₂ O	-653.007318	0.219528	0.232584	108.7	≡ 0
<i>o</i> - ³ 1•H ₂ O	-652.953977	0.216425	0.229886	112.8	31.8
<i>m</i> -1•H ₂ O	-652.971934	0.217936	0.231323	110.3	21.4
<i>m</i> - ³ 1•H ₂ O	-652.952737	0.215558	0.229338	114.5	32.2
<i>p</i> -1•H ₂ O	-652.999717	0.218711	0.232280	111.7	4.6
<i>p</i> - ³ 1•H ₂ O	-652.941476	0.214545	0.228889	119.9	39.0

^a Thermal enthalpy correction including zero-point energy.

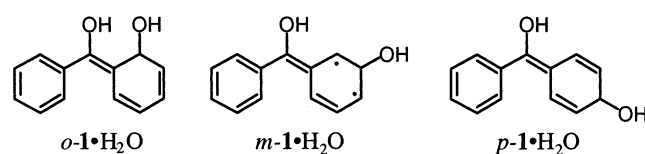
at still higher concentrations. The transient was no longer detectable at acid concentrations of 6 M or higher.

The temperature dependence of the decay of 1•H₂O in 0.1 M HClO₄ was determined in the range of 25–57 °C (10 data points). Activation parameters $E_a = 18.5 \pm 0.2$ kcal mol⁻¹ and $A = (5.5 \pm 1.4) \times 10^{12}$ s⁻¹ were obtained from an Arrhenius plot. The decay rate constant of 1•H₂O in 0.1 M aqueous HClO₄ at -5.9 °C was $(3.2 \pm 0.4) \times 10^{-3}$ s⁻¹ (three measurements). Product 1•H₂O could be extracted to pentane after irradiation of 1 at -6 °C in aqueous HClO₄. Its decay rate constant in pentane, measured by the absorbance decrease with time at 310 nm, was quite similar to that in aqueous solution, $k = (3.1 \pm 1.6) \times 10^{-3}$ s⁻¹ (three measurements, -5.9 °C). These experiments show that 1•H₂O is a neutral compound and that its decay rate is hardly solvent-dependent. However, the decay rate of 1•H₂O in water increased with acid concentrations exceeding 1 M (Table 1).

Photoacoustic Calorimetry. Solutions of 1 and HClO₄ (4 M) in a mixture of acetonitrile (30% by volume) and water were excited at 248 nm. Acetonitrile was added to increase the thermal expansion coefficient of the solvent. Optical LFP of 1 in 4 M aqueous HClO₄ indicated that the intermediate ³1•H₂O was formed within the duration of the laser pulse and decayed with a lifetime of 42 ± 1 ns. Consistently, the photoacoustic waves indicated that a time-resolved heat deposition process occurred with a similar lifetime. The best fit was obtained with a biexponential function for the heat release. The rate constant for the fast processes, which occur rapidly on the time scale of the duration of the laser pulse, was arbitrarily fixed to 1 ns. Three parameters were adjusted, the two amplitudes of the two heat deposition processes and the rate constant for the time-resolved process. Of the total energy (248 nm \Rightarrow 115.2 kcal per mole of photons absorbed), $57.5 \pm 4.3\%$ was released within 1 ns and $34 \pm 6\%$ with a lifetime of 45 ± 7 ns. The goodness-of-fit was excellent and was not improved by using three exponentials in the kinetic trial function. Hence, the decay of ³1•H₂O deposits 39 ± 7 kcal mol⁻¹.

In a second series of experiments, more dilute acid (0.17 M HClO₄, 30% acetonitrile) was used. Optical LFP of this mixture gave a lifetime of 32 ± 5 ns for ³1 and 52 ± 5 ns for ³1•H₂O. On the basis of purely statistical criteria, the fits to the acoustic waves were equally acceptable with a bi- or triexponential function. The fit parameters obtained with a triexponential function were chosen, because that was required by the analysis of the LFP data. The first exponential, formation of ³1, was fixed to occur with $\tau = 1$ ns and to release 46.2 kcal mol⁻¹ (115.2 kcal mol⁻¹ - $E_T(1)$). In the delayed heat evolution, $16.5 \pm 6.4\%$ of the absorbed energy was deposited with $\tau = 25 \pm 10$ ns and $30 \pm 7\%$ with $\tau = 55 \pm 15$ ns. Thus, proton-catalyzed adiabatic hydration of ³1 yielding ³1•H₂O affords 19 ± 7 kcal mol⁻¹, and the decay of ³1•H₂O releases another 34.5 ± 8.0 kcal mol⁻¹. The average of the two measurements (4 and 0.17 M HClO₄) for this process is 37 ± 6 kcal mol⁻¹. No corrections were made for reaction volumes.

Density Functional Calculations. The energies of three possible structures of hydrate 1•H₂O in the ground state and in the lowest triplet state were calculated using the B3LYP density functional with the 6-31G* basis set, as provided in the Gaussian 98²⁴ program package. All structures were fully optimized, and frequency calculations were done. The energies given in Table 2 are those of the most stable conformers (OH bonds) and *E/Z* isomers shown below.



From the last column of Table 2, it is seen that the ortho isomer is the most stable hydrate in the ground state. In the triplet state, the energies of the ortho and the meta isomers are similar, that of the para isomer is higher. The calculated triplet excitation energies (0 K) of the three isomers are $E_T(\text{ortho}) = 31.5$, $E_T(\text{meta}) = 10.6$, and $E_T(\text{para}) = 33.6$ kcal mol⁻¹. The triplet energy of 1 was calculated as $E_T = 61.5$ kcal mol⁻¹ by the same method. The enthalpy of dehydration (298 K) of *o*-1•H₂O to 1 + H₂O is calculated as $\Delta_r H = -23.8$ kcal mol⁻¹.

Energy Transfer to Biacetyl. The triplet energy of protonated triplet benzophenone, $E_T(^3\text{1H}^+) = 61.8$ kcal mol⁻¹,⁴ is known from phosphorescence measurements in strongly acidic media. With $E_T(\text{biacetyl}) = 56.4$ kcal mol⁻¹,²⁵ it should be possible to observe energy transfer to biacetyl from both ³1 and ³1H⁺. The triplet-triplet absorption maxima of biacetyl are at 315 ($\epsilon \approx 6000$ M⁻¹ cm⁻¹) and 800 nm.²⁶ LFP of 1 (3×10^{-5} M, excitation at 248 nm) in neutral, aerated water with added biacetyl (0–0.01M) showed accelerated first-order decay of ³1 at 520 nm and biexponential decay at 325 nm. The fast component observed at 325 nm was attributed to the accelerated decay of ³1, and the slow one was attributed to the decay of triplet biacetyl formed by energy transfer. A resolved growth followed by a decay of absorbance was seen at 800 nm, where only triplet biacetyl absorbs. The observed rate of energy transfer increased linearly with increasing biacetyl concentration. The best traces were obtained by monitoring at 520 nm (seven data points, 0–0.05 M biacetyl). A least-squares fit gave $k_{\text{et}} = (1.0 \pm 0.1) \times 10^9$ M⁻¹ s⁻¹ for the bimolecular rate constant of energy transfer from ³1 to biacetyl.

In previous work,^{5,8} the transient observed by LFP of 1 in 1 M aqueous HClO₄ has been attributed to ³1H⁺. Addition of up to 0.05 M biacetyl failed to accelerate the decay of the transient absorbance at 500 nm, which supports our proposal that this species is not ³1H⁺ but ³1•H₂O. The triplet energies of the three isomers of ³1•H₂O (Table 2) were calculated to be well below that of biacetyl.

To demonstrate energy transfer from ³1H⁺ to biacetyl, the experiment was repeated using acidified acetonitrile (1 M

TABLE 3: Proton Quenching Rate Constants, Transient Absorption Spectra, and Lifetimes for Various Derivatives of **1** and **2**

compd	$k_{\text{obs,H}^+}$ ($10^7 \text{ M}^{-1} \text{ s}^{-1}$)	$\lambda_{\text{max}}(^3\mathbf{1}\cdot\text{H}_2\text{O})$ (nm)	$\tau(^3\mathbf{1}\cdot\text{H}_2\text{O})$ (ns)	$\lambda_{\text{max}}(\mathbf{1}\cdot\text{H}_2\text{O})$ (nm)	$\tau(\mathbf{1}\cdot\text{H}_2\text{O})^a$ (s)
benzophenone (1)	38 ± 1	320, 500	50	315	5.4 ± 1.0
3-methylbenzophenone	9.0 ± 0.1	320, 510	60	320	22.7 ± 0.8
4-methylbenzophenone	62 ± 2	320, 510	50	315	8.6 ± 0.5
3,4-dimethylbenzophenone	6.8 ± 0.2	<340, 515	50	320	8.0 ± 1.1
3,5-dimethylbenzophenone	7.2 ± 0.2	320, 510	60	320	22.6 ± 0.9
4-aminobenzophenone	60 ± 2	315, 505	80	315	8.3 ± 0.8
4,4'-difluorobenzophenone	1.3 ± 0.2	320, 500	50	305	0.15 ± 0.02
acetophenone (2)	22 ± 1			280	0.9 ± 0.1
2-chloroacetophenone	52 ± 1			285	3.3 ± 0.5
2-fluoroacetophenone	93 ± 2			280	0.05 ± 0.01
4-fluoroacetophenone	1.0 ± 0.1			280	0.06 ± 0.01
3-trifluoromethylacetophenone	0.88 ± 0.03			285	0.55 ± 0.03

^a Aqueous 0.1 M HClO₄; derivatives of **2** required addition of 10% acetonitrile, and derivatives of **1** required 20% acetonitrile to achieve sufficient solubility.

HClO₄) as a medium, in which hydration of ³1H⁺ does not interfere. Biacetyl was unstable in this medium, and its absorption band at 415 nm decayed with a half-life of 7 min. Thus, biacetyl was added immediately prior to LFP of **1** (1.5×10^{-5} M). The lifetime of ³1H⁺ (440 ns in air-saturated solution, measured at 315 nm) was reduced to 57 ns by the addition of 5×10^{-3} M biacetyl, i.e., the rate constant for energy transfer from ³1H⁺ to biacetyl amounts to $k_{\text{et}} \approx 3.0 \times 10^9 \text{ M}^{-1} \text{ s}^{-1}$ in this solvent.

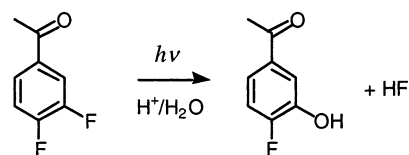
Attempts to Detect 1·H₂O by ¹H NMR. Several attempts were made to detect the long-lived product **1**·H₂O by ¹H NMR. These experiments were hampered by the low yield of intermediate **1**·H₂O²⁷ and by the fact that **1**·H₂O was, itself, quite sensitive to irradiation and could not be accumulated to a high extent even at reduced temperature. The best results were obtained by irradiation of **1** (6×10^{-3} M) in acidic D₂O/CD₃OD 1:1 (0.3 M DCIO₄) with 50 248-nm laser pulses at -30 °C in a quartz NMR tube. At this temperature, the lifetime of **1**·H₂O, monitored by its absorbance at 310 nm, was about 2 h. Following irradiation, the solution was quickly transferred to a cooled (-30 °C) 500 MHz NMR spectrometer, and the spectra were accumulated. Apart from the strong signals due to **1**, very weak signals were detected, which disappeared irreversibly on warming. The spectrum is given as Supporting Information.

Isotope Exchange. Solutions of **1** in acidic D₂O (0.25 M D₂SO₄) were irradiated with 5000 248-nm pulses from an excimer laser. No deuterium incorporation was detected by gas chromatography/mass spectrometry (GC/MS) and ¹H NMR analysis of the irradiated sample. The dose was sufficient to excite each solute molecule about 1000 times.

LFP of **2 and Derivatives of **1** and **2**.** A brief study of **2** and several derivatives of **1** and **2** by LFP indicated that the triplet state of these compounds is also quenched by protons. The observed bimolecular quenching rate constants $k_{\text{obs,H}^+}$ are collected in Table 3 and interpreted in the discussion (see eq 7). Acid quenching of ³2 did not produce a transient similar to ³1·H₂O, only a weak, long-lived transient, $\lambda_{\text{max}} \approx 280$ nm, $\tau = 0.9$ s, presumably due to the *ortho*-hydrate **2**·H₂O. The lifetime of the triplet hydrate formed from **2**, ³2·H₂O, appears to be less than 20 ns. *m*-Fluoroacetophenone in 1 M HClO₄ did produce a strong transient absorption, $\lambda_{\text{max}} \approx 350$ nm, $\tau = 50$ ns. Permanent absorbance was left in the range of 300–350 nm, $\lambda_{\text{max}} = 308$ nm, after the decay of this transient (cf. next section).

As observed with **1**·H₂O, the yield of **2**·H₂O increased with acid concentration in dilute aqueous HClO₄. Linear regression of $1/A_0$ (280 nm) vs $1/[\text{H}^+]$ ($[\text{H}^+] = 0.001\text{--}0.10$ M) gave an intercept of 4.40 ± 0.05 and a slope of $(1.69 \pm 0.05) \times 10^{-2}$ M.

SCHEME 1: Photohydrolysis of 3,4-Difluoroacetophenone in Aqueous Acid

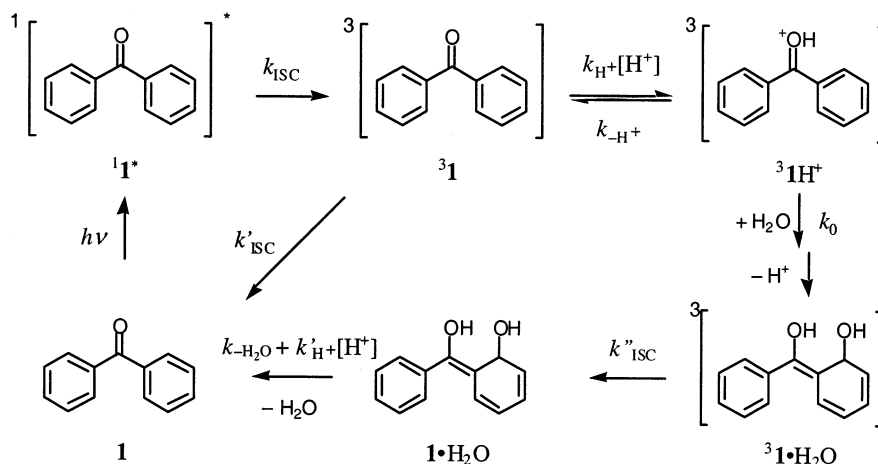


Preparative Work and Quantum Yields of Photohydrolysis. Irradiation of 3-fluoroacetophenone in aqueous acid produced a new absorption band at 305 nm. Addition of excess base shifted the absorption maximum of the photoproduct to 343 nm. The shapes and maxima of these spectra were nearly identical to those of authentic 3-hydroxyacetophenone: $\lambda_{\text{max}} = 308$ nm in aqueous acid, 348 nm in base. This indicated essentially clean photosubstitution of the fluoride. Similarly, irradiation of 3,3'-difluorobenzophenone produced a new band at 310 nm (370 nm in base). The photoproduct formed by irradiation of 3,4-difluoroacetophenone (Scheme 1) in aqueous acid was identified as 4-fluoro-3-hydroxyacetophenone (Experimental Section).

Quantum yields of photohydrolysis were measured spectrophotometrically at low conversions in degassed 0.1 M aqueous HClO₄, assuming clean conversion to the corresponding phenols. They were high for derivatives carrying a *meta*-fluoro substituent: $\phi \approx 0.5$ (3-fluoroacetophenone, deviations from the initial isobestic points indicated secondary photolysis), $\phi = 0.63 \pm 0.10$ (3,4-difluoroacetophenone), and $\phi = 0.7 \pm 0.1$ (3,3'-difluorobenzophenone). Photohydrolysis was not observed in neutral aqueous solutions: $\phi < 0.01$. 2-Fluoroacetophenone reacted more slowly upon irradiation in aqueous acid, $\phi \approx 0.2$, and the spectral changes were not consistent with a clean formation of 2-hydroxyacetophenone. In addition to a band at 323 nm, expected for 2-hydroxyacetophenone, a broad band extending to the visible was formed. 4-Fluoroacetophenone decomposed very slowly upon irradiation in aqueous acid. There was no indication for the formation of 4-hydroxyacetophenone $\lambda_{\text{max}} = 275$ nm, $\phi < 0.01$.

Discussion

pH Rate Profiles and Assignment of Transient Intermediates. Five different transient intermediates are formed by excitation of **1** in aqueous acid. They were identified by their absorption spectra and assigned to the intermediates ¹1, ³1, ³1H⁺, ³1·H₂O, and **1**·H₂O as shown in Scheme 2. The observed transient kinetics gave five first-order rate constants, $k_1\text{--}k_5$, Table 1. A reliable determination of five rate constants

SCHEME 2: Postulated Reaction Sequence for the Photohydration of **1** in Aqueous Acid^a

^a The structure shown for ³**1**·H₂O is one of several possible isomers (cf. Scheme 3 below).

TABLE 4: Absorption Maxima (Relative Intensities) of the Five Transient Intermediates Formed by Flash Photolysis of **1 in Aqueous Acid**

assignment	λ_{\max} (nm) (relative intensity)	spectrum
1	335 (1), 575 (ca. 0.3)	Figures 2, 3, and 5 (initial spectra)
³ 1	330 (1), 525 (ca. 0.9)	Figure 2 (last spectrum)
³ 1H ⁺	320 (1), 385 (ca. 0.8), 500 (ca. 0.7)	Figure 7 (10 ns delay)
³ 1 ·H ₂ O	320 (1), 500 (ca. 0.2)	Figure 6 (10 ns delay)
1 ·H ₂ O	315	broad Gaussian band (not shown)

from transient absorption measurements is rarely possible. The present analysis was feasible, because the observed processes have quite different lifetimes spanning a time scale of 12 orders of magnitude and because the rates of these processes smoothly followed the pH dependencies expected from Scheme 2.

Identification of the first two intermediates, ¹**1** and ³**1**, is straightforward. The initial absorption bands recorded immediately after excitation with a subpicosecond pulse at 248 nm (Figures 2, 3, 5; Table 4) are attributed to S₁–S₀ transitions of the excited singlet state of **1**, ¹**1**. The visible absorption band of ¹**1** ($\lambda_{\max} = 575$ nm in acetonitrile) has been observed previously.^{28,29} The first absorption changes are due to ISC of ¹**1** yielding the well-known triplet–triplet absorption of benzophenone, ³**1**, $\lambda_{\max} = 330$ and 525 nm.^{4,26} The lifetime of ¹**1** in aqueous solution is 6.5 ps. The ISC quantum yield of **1** is very close to unity,²⁵ so that the observed rate constant of this process, $k_1 = (1.55 \pm 0.09) \times 10^{11} \text{ s}^{-1}$, may be equated to the rate constant of ISC to the triplet state, k_{ISC} . In aqueous acid (≥ 1 M), a small amount of protonation occurs in competition to ISC of ¹**1**. The adiabatic formation of ¹**1H**⁺ was detected by fluorescence spectroscopy (Figure 1).

The lifetime of ¹**1** in acetonitrile has been determined previously: $^1\tau = 9 \pm 2^{28}$ and 9.6 ± 0.9 ps.²⁹ Singlet–triplet ISC to the n,π^* triplet state of **1** appears to be accelerated by H-bonding. In remarkable contrast, H-bonding solvents reduce the rate of ISC to the π,π^* triplet state of *p*-hydroxyacetophenone.³⁰ The similarity between the π,π^* absorption spectra of ³**1** and benzophenone ketyl radical has been noted long ago.³¹ It was attributed to the fact that both species have the same π system bearing a single unpaired electron. For the same reason, the excited singlet state ¹**1** also has a similar absorption spectrum.

Assignment of the next three transients, the protonated triplet of **1**, ³**1H**⁺, its hydration product, ³**1**·H₂O, and the long-lived ground state intermediate **1**·H₂O, requires more detailed argumentation. We begin with an analysis of the kinetic system defined by Scheme 2. The proposed mechanism comprising five reactive intermediates and the end product **1** gives a set of six coupled differential equations. As protons are in large excess relative to the amount of the transient intermediates formed, [H⁺] may be assumed to be constant during the transient decays, and the products $k_{\text{H}^+}[\text{H}^+]$ and $k'_{\text{H}^+}[\text{H}^+]$ can be treated as first-order rate constants. All reactions are then first order, which results in a rate law for the time-dependent absorbances *A* consisting of five observable exponentials, eq 1.

$$A(\lambda, t) = A_0(\lambda, \infty) + \sum_{i=1,5} A_i e^{-k_i t} \quad (1)$$

The relations between the observable rate constants k_1 – k_5 and the microscopic rate constants shown in Scheme 2 were determined by standard methods of linear algebra,³² eqs 2–6.

$$k_1 = k_{\text{ISC}} \quad (2)$$

$$k_2 = \frac{\alpha + \sqrt{\alpha^2 - 4\beta}}{2} \quad (3)$$

$$k_3 = \frac{\alpha - \sqrt{\alpha^2 - 4\beta}}{2} \quad (4)$$

where $\alpha = k_{\text{H}^+}[\text{H}^+] + k_{-\text{H}^+} + k_0 + k'_{\text{ISC}}$ and $\beta = k_{\text{H}^+}[\text{H}^+]k_0 + k_{-\text{H}^+}k'_{\text{ISC}} + k_0k'_{\text{ISC}}$.

$$k_4 = k''_{\text{ISC}} \quad (5)$$

$$k_5 = k_{-\text{H}_2\text{O}} + k'_{\text{H}^+}[\text{H}^+] \quad (6)$$

Of the five observable rate constants, k_2 , k_3 , and k_5 are functions of the proton concentration [H⁺]. Nonlinear least-squares fits of eqs 2–6 to the experimental rate data (Table 1) are shown in Figure 8. The resulting fit parameters, k_{ISC} , k'_{ISC} , k''_{ISC} , k_{H^+} , $k_{-\text{H}^+}$, k_0 , $k_{-\text{H}_2\text{O}}$, and k'_{H^+} , are collected in Table 5.

Several observations clearly indicate that the transient intermediate ³**1**·H₂O formed in aqueous acid is a hydrate, not the conjugate acid of ³**1**: (i) The absorption spectrum of ³**1**·H₂O is substantially different from that of ³**1H**⁺, which is observed in

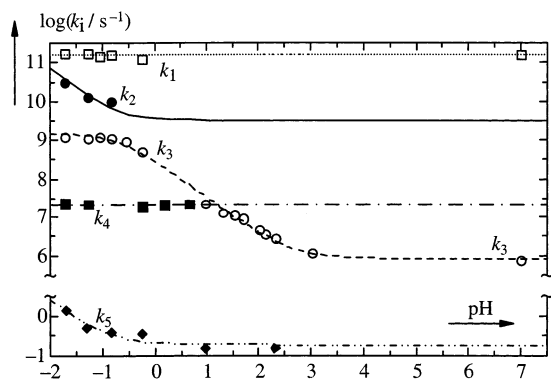


Figure 8. pH rate profiles of the observed rate constants k_1 (\blacktriangledown), k_2 (\bullet), k_3 (\circ), k_4 (\blacksquare), and k_5 (\blacklozenge) given in Table 1. The lines were obtained by nonlinear least-squares fitting of eqs 2–6 to the data points. The resulting microscopic rate constants are given in Table 5.

TABLE 5: Microscopic Rate Constants Determined by Fitting the Parameters of Eq 2–6 to the Observed Rate Constants Given in Table 1

reaction	rate constant
${}^1\mathbf{1} \rightarrow {}^3\mathbf{1}$	$k_{\text{ISC}} = (1.55 \pm 0.09) \times 10^{11} \text{ s}^{-1}$
${}^3\mathbf{1} + \text{H}^+ \rightarrow {}^3\mathbf{1H}^+$	$k_{\text{H}^+} = (6.8 \pm 0.9) \times 10^8 \text{ M}^{-1} \text{ s}^{-1}$
${}^3\mathbf{1H}^+ \rightarrow {}^3\mathbf{1} + \text{H}^+$	$k_{-\text{H}^+} = (1.8 \pm 0.5) \times 10^9 \text{ s}^{-1}$
${}^3\mathbf{1H}^+ + \text{H}_2\text{O} \rightarrow {}^3\mathbf{1}\cdot\text{H}_2\text{O} + \text{H}^+$	$k_0 = (1.5 \pm 0.2) \times 10^9 \text{ s}^{-1}$
${}^3\mathbf{1} \rightarrow \mathbf{1}$	$k'_{\text{ISC}} = (8 \pm 2) \times 10^5 \text{ s}^{-1} (a)$
${}^3\mathbf{1}\cdot\text{H}_2\text{O} \rightarrow \mathbf{1}\cdot\text{H}_2\text{O}$	$k''_{\text{ISC}} = (2.13 \pm 0.08) \times 10^7 \text{ s}^{-1}$
$\mathbf{1}\cdot\text{H}_2\text{O} \rightarrow \mathbf{1} + \text{H}_2\text{O}$	$k_{-\text{H}_2\text{O}} = 0.19 \pm 0.03 \text{ s}^{-1}$
$\mathbf{1}\cdot\text{H}_2\text{O} + \text{H}^+ \rightarrow \mathbf{1} + \text{H}_3\text{O}^+$	$k'_{\text{H}^+} = 0.024 \pm 0.006 \text{ M}^{-1} \text{ s}^{-1}$

^a The value determined in neutral, air-saturated solution is $k'_{\text{ISC}} = (7.3 \pm 0.1) \times 10^5 \text{ s}^{-1}$. The rate is dominated by oxygen-induced quenching. The other rate constants were not affected by degassing.

solvents of low water activity. (ii) The kinetic analysis (Table 5) shows that hydration of ${}^3\mathbf{1H}^+$ is faster than the preceding protonation of ${}^3\mathbf{1}$ in moderately concentrated aqueous acid. Therefore, intermediate ${}^3\mathbf{1H}^+$ is not detected under these conditions. (iii) The triplet energy of ${}^3\mathbf{1}\cdot\text{H}_2\text{O}$ is insufficient for energy transfer to biacetyl, $E_{\text{T}} = 56.4 \text{ kcal mol}^{-1}$. However, energy transfer to biacetyl does occur, as expected, in acidified acetonitrile, where ${}^3\mathbf{1H}^+$ is the intermediate formed by protonation of ${}^3\mathbf{1}$.

Prolonged irradiation of $\mathbf{1}$ in acidic D_2O did not lead to any deuterium incorporation. Hence, quenching of ${}^3\mathbf{1}$ cannot be attributed to protonation of the aromatic rings, which is responsible for acid quenching of many excited aromatic compounds.³³ The unusual Arrhenius parameters determined from the temperature dependence of the rate constant $k_4 = k'_{\text{ISC}}$ in 1 M HClO_4 , $A = (1.6 \pm 0.4) \times 10^8 \text{ s}^{-1}$ and $E_{\text{a}} = 1.13 \pm 0.10 \text{ kcal mol}^{-1}$, indicate that the decay of ${}^3\mathbf{1}\cdot\text{H}_2\text{O}$ is a spin-forbidden process.

Structure of the Transient Intermediates ${}^3\mathbf{1}\cdot\text{H}_2\text{O}$ and $\mathbf{1}\cdot\text{H}_2\text{O}$, Photohydrolysis of Fluorinated Derivatives of $\mathbf{1}$ and $\mathbf{2}$. The above considerations led us to conclude that rapid water addition to ${}^3\mathbf{1H}^+$ is responsible for proton quenching of ${}^3\mathbf{1}$. This hypothesis suggested that derivatives with a leaving group on the phenyl ring might undergo irreversible photosubstitution reactions in aqueous acid. That was found to be the case: *meta*-fluoro derivatives of $\mathbf{1}$ and $\mathbf{2}$ underwent essentially clean and efficient ($\phi \approx 0.6$) photohydrolysis in aqueous acid (Scheme 1). *ortho*-Fluoroacetophenone reacted more slowly ($\phi \approx 0.2$), and *para*-fluoroacetophenone was essentially inert to irradiation ($\phi < 0.01$). No such reaction was observed in neutral aqueous solution. These findings indicate that water adds predominantly

to the *meta* position and, to a lesser extent, to the *ortho* position. Density functional theory calculations for the three isomeric hydrates of $\mathbf{1}$ predicted that the *meta* isomer is slightly favored over the *ortho* isomer in the triplet state, both energies being well below that of the *para* isomer (Table 2). The high quantum yields ($\phi \approx 0.6$) of photosubstitution of the *meta*-fluoro derivatives also show that water addition to *meta* positions carrying a fluoro substituent is preferred over unsubstituted *meta* positions and, not surprisingly, that fluoride elimination in the *ipso*-hydrate prevails over hydroxyde elimination. Relying mainly on the photochemistry of the fluorinated derivatives, we tentatively assign the observed transient ${}^3\mathbf{1}\cdot\text{H}_2\text{O}$ ($\tau = 47 \text{ ns}$) to the *meta* isomer.

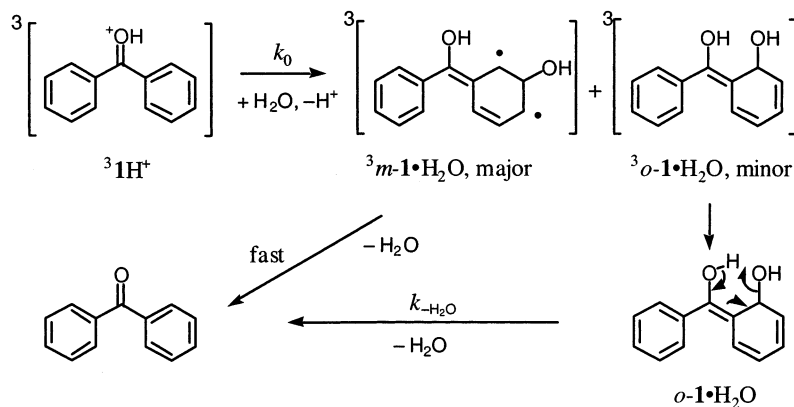
The long-lived transient $\mathbf{1}\cdot\text{H}_2\text{O}$ ($\lambda_{\text{max}} = 315 \text{ nm}$) that is left after the decay of ${}^3\mathbf{1}\cdot\text{H}_2\text{O}$ is a minor product.²⁷ Its properties are consistent with assignment to the *ortho*-hydrate, 6-(hydroxyphenyl-methylene)cyclohexa-2,4-dien-1-ol (Scheme 3). Intermediate $\mathbf{1}\cdot\text{H}_2\text{O}$ is a neutral compound; it can be extracted from water to pentane, and its lifetime is about 5 min at $-6 \text{ }^\circ\text{C}$ in both solvents. Replacement of the methyl group in $\mathbf{2}\cdot\text{H}_2\text{O}$ by phenyl in $\mathbf{1}\cdot\text{H}_2\text{O}$ is accompanied by a 35 nm red shift, proving that the second phenyl group is in conjugation with the π chromophore of $\mathbf{1}\cdot\text{H}_2\text{O}$. More O'Ferrall and co-workers have measured rate constants for acid-catalyzed dehydration of hydrates of several aromatic compounds.³⁴ The rate constant for acid-catalyzed dehydration of $\mathbf{1}\cdot\text{H}_2\text{O}$, $k'_{\text{H}^+} = 0.024 \text{ M}^{-1} \text{ s}^{-1}$ (Table 5), is comparable to that reported for, e.g., 1-hydroxy-1,2-dihydronaphthalene, $k_{\text{H}^+} = 0.35 \text{ M}^{-1} \text{ s}^{-1}$. On the other hand, the pH-independent dehydration reactions observed here, $k_{-\text{H}_2\text{O}}(\mathbf{1}\cdot\text{H}_2\text{O}) = 0.19 \text{ s}^{-1}$ and $k_{-\text{H}_2\text{O}}(\mathbf{2}\cdot\text{H}_2\text{O}) = 1.1 \text{ s}^{-1}$ (Table 3), are without precedent. The fact that a similar rate is observed when $\mathbf{1}\cdot\text{H}_2\text{O}$ is extracted to pentane indicates that dehydration is assisted by the neighboring enol function, which transfers a proton to the leaving OH group. This is consistent only with $\mathbf{1}\cdot\text{H}_2\text{O}$ and $\mathbf{2}\cdot\text{H}_2\text{O}$ being the *ortho*-hydrates.

No intermediate attributable to the *meta*-hydrate in the ground state was detected by LFP of $\mathbf{1}$ or $\mathbf{2}$; its lifetime is presumably much shorter than that of the *ortho* isomer. Indeed, LFP of *m*-fluoroacetophenone in 1 M HClO_4 showed that the photo-product, *m*-hydroxyacetophenone, is present immediately after the decay of the transient attributed to the triplet hydrate, $\tau = 50 \text{ ns}$. The reaction enthalpy of $37 \pm 6 \text{ kcal mol}^{-1}$, which is associated with the decay of ${}^3\mathbf{1}\cdot\text{H}_2\text{O}$ as determined by photoacoustic calorimetry, then represents the reaction ${}^3m\text{-}\mathbf{1}\cdot\text{H}_2\text{O} \rightarrow \mathbf{1} + \text{H}_2\text{O}$.

Steady State Analysis of Proton Quenching in Dilute Acid. For low acid concentrations, $[\text{H}^+] < 0.01 \text{ M}$, protonation of ${}^3\mathbf{1}$ is the rate-limiting step preceding hydration, and the steady state approximation can be used for ${}^3\mathbf{1H}^+$, i.e., $d[{}^3\mathbf{1H}^+]/dt = k_{\text{H}^+}[\text{H}^+][{}^3\mathbf{1}] - (k_0 + k_{-\text{H}^+})[{}^3\mathbf{1H}^+] \approx 0$. This leads to a simplified expression for the third observable rate constant, eq 7.

$$k_3 \approx k'_{\text{ISC}} + k_{\text{H}^+}k_0[\text{H}^+]/(k_0 + k_{-\text{H}^+}) = k'_{\text{ISC}} + k_{\text{obs,H}^+}[\text{H}^+] \quad (7)$$

Note that the observed second-order constant rate for proton quenching of ${}^3\mathbf{1}$ in dilute acid ($\text{pH} > 2$), $k_{\text{obs,H}^+}$, is lower than the rate constant for protonation of ${}^3\mathbf{1}$ by the factor $f = k_0/(k_0 + k_{-\text{H}^+}) = 0.45 \pm 0.10$, which represents the fraction of ${}^3\mathbf{1H}^+$ that is quenched by water addition in dilute acid. Least-squares fitting of eq 7 gave $k_{\text{obs,H}^+} = (3.8 \pm 0.1) \times 10^8 \text{ M}^{-1} \text{ s}^{-1}$, in reasonable agreement with the less accurate value of $(6.4 \pm 1.3) \times 10^8 \text{ M}^{-1} \text{ s}^{-1}$ that Porter and Ledger³ had determined by phosphorescence quenching. The quantum yield for the formation of ${}^3\mathbf{1}\cdot\text{H}_2\text{O}$ in dilute acid is then given by $\phi_{\text{hydr}} = k_{\text{obs,H}^+}$

SCHEME 3: Tentative Assignment of Intermediates ${}^3\mathbf{1}\cdot\text{H}_2\text{O}$ and $\mathbf{1}\cdot\text{H}_2\text{O}$ 

$[\text{H}^+]/(k_{\text{obs,H}^+}[\text{H}^+]f + k'_{\text{ISC}})$. Hence, the inverse yield of $\mathbf{1}\cdot\text{H}_2\text{O}$ should be linearly related to the inverse of $[\text{H}^+]$ in dilute acid, eq 8. The initial absorbance, A_0 (315 nm), by the long-lived transient $\mathbf{1}\cdot\text{H}_2\text{O}$ accurately obeyed eq 8 for acid concentrations in the range of 0.001–0.10 M.

$$1/A_0 \approx a + ak'_{\text{ISC}}/k_{\text{obs,H}^+}[\text{H}^+] \quad (8)$$

The ratio of slope and intercept of eq 8 (determined by linear regression; see Results, Conventional Flash Photolysis), $k'_{\text{ISC}}/k_{\text{obs,H}^+} = (1.95 \pm 0.01) \times 10^{-3}$ M, is in excellent agreement with the ratio of the individual rate constants k'_{ISC} (Table 5, footnote a) and $k_{\text{obs,H}^+}$ (Table 3) determined independently, $k'_{\text{ISC}}/k_{\text{obs,H}^+} = (1.92 \pm 0.06) \times 10^{-3}$ M. The quantitative agreement between these two results confirms that transient $\mathbf{1}\cdot\text{H}_2\text{O}$ results from proton quenching of ${}^3\mathbf{1}$. Similarly, $k'_{\text{ISC}}/k_{\text{obs,H}^+} = (3.84 \pm 0.12) \times 10^{-3}$ M was obtained from the ratio of slope to intercept of the corresponding plot for the initial absorbance A_0 (280 nm) by the transient $\mathbf{2}\cdot\text{H}_2\text{O}$ and $k'_{\text{ISC}}/k_{\text{obs,H}^+} = (3.4 \pm 0.3) \times 10^{-3}$ from the individual rate constants. This result corroborates our assumption that the same mechanism (Schemes 2 and 3) applies for $\mathbf{2}$, although ${}^3\mathbf{2}\cdot\text{H}_2\text{O}$ escaped detection by nanosecond LFP.

Acidity of $\mathbf{1H}^+$ in the Electronic Ground State and in the Lowest Excited Singlet and Triplet States. The ratio of the rate constants for adiabatic dissociation of ${}^3\mathbf{1H}^+$, $k_{-\text{H}^+}$, and protonation of ${}^3\mathbf{1}$, k_{H^+} , provides the acidity constant of $\mathbf{1}$ in the excited triplet state: $K_{\text{a}}({}^3\mathbf{1H}^+) = k_{-\text{H}^+}/k_{\text{H}^+} = 2.65 \pm 0.66$, $\text{p}K_{\text{a}}({}^3\mathbf{1H}^+) = -0.4 \pm 0.1$. The rate constants $k_{-\text{H}^+}$ and k_{H^+} (Table 5) were determined from the kinetic data obtained in strongly acidic solutions, $H_0 = -0.25$ to -1.7 . The resulting acidity constant is, strictly, a concentration quotient determined over a substantial range of (high) ionic strengths. However, dissociation of ${}^3\mathbf{1H}^+$ to ${}^3\mathbf{1}$ and H^+ is a charge shift reaction, which should not depend much on ionic strength. Both $k_{-\text{H}^+}$ and k_{H^+} are substantially slower than expected³⁵ for proton transfer between two oxygen atoms, i.e., “normal” acids and bases. This unusual finding may be attributed to the fact that the electronic wave functions of ${}^3\mathbf{1}$ (${}^3n,\pi^*$) and of ${}^3\mathbf{1H}^+$ (${}^3\pi,\pi^*$) have different symmetry (assuming planar structures), so that adiabatic proton transfer to ${}^3\mathbf{1}$ encounters a symmetry-imposed barrier.

Depending on the acidity function used, values for the acidity constant of protonated benzophenone ranging from $\text{p}K_{\text{a}}(\mathbf{1H}^+) = -6.2$ to -4.7 have been reported. We adopt the more recent estimates based on the H_0 acidity function $\text{p}K_{\text{a}}(\mathbf{1H}^+) = -4.74^5$ and -4.71 .³⁶ The acidity constant of $\mathbf{1H}^+$ in the lowest excited singlet state may then be estimated by the Förster cycle, $\text{p}K_{\text{a}}({}^1\mathbf{1H}^+) \approx \text{p}K_{\text{a}}(\mathbf{1H}^+) + \Delta\tilde{\nu}_{0-0}/(2.3RT)$. Using

$\text{p}K_{\text{a}}(\mathbf{1H}^+) = -4.7$,³⁶ $\tilde{\nu}_{0-0}({}^1\mathbf{1}) = 26\,040\text{ cm}^{-1}$,²⁵ and $\tilde{\nu}_{0-0}({}^1\mathbf{1H}^+) = 24\,250\text{ cm}^{-1}$ estimated from Figure 1, we obtain $\text{p}K_{\text{a}}({}^1\mathbf{1H}^+) \approx -1$. On the basis of the older value $\text{p}K_{\text{a}}(\mathbf{1H}^+) = -5.7$ and somewhat different estimates of the excitation energies $\tilde{\nu}_{0-0}$, Ireland and Wyatt⁴ estimated $\text{p}K_{\text{a}}({}^1\mathbf{1H}^+) \approx -3.6$. We detected adiabatic protonation of $\mathbf{1}$ by fluorescence emission from ${}^1\mathbf{1H}^+$ following excitation of $\mathbf{1}$ in solutions with acid concentrations exceeding 1 M. This indicates that the latter estimate is low.

Comments on Previous Studies. Favaro and Bufalini⁶ have studied the pH dependence of energy transfer from ${}^3\mathbf{1}$ to biacetyl by phosphorescence. By steady state analysis of the phosphorescence intensities, they obtained a lifetime of 2.3×10^{-4} s for ${}^3\mathbf{1}$ in degassed, neutral, aqueous solution (extrapolated to infinite dilution of $\mathbf{1}$) and a lifetime of ca. 40 ns for the triplet species formed in acidic solution ($\text{pH} < 1$).³⁷ That species was attributed to an “excited complex” different from protonated benzophenone in the triplet state, ${}^3\mathbf{1H}^+$. This assignment comes remarkably close to that made in the present study. It was based on the previous³⁸ observation that the phosphorescence emission at 77 K from frozen aqueous solutions of pH 3 to $H_0 -4$ was different from that of frozen 70% HClO_4 or 96% H_2SO_4 , where protonation of $\mathbf{1}$ to ${}^3\mathbf{1H}^+$ occurs in the ground state. However, Rayner and co-workers⁷ subsequently showed that the differences of the phosphorescence spectra noted by Favaro and Bufalini cannot be taken as evidence for a benzophenone–hydroxonium complex, because similar changes were found by addition of sodium acetate. The shift was attributed to an effect of the additive (acid or salt) on the frozen solvent structure.

Both Wyatt and co-workers^{4,5} and Shizuka and co-workers^{8,11} have assumed that the transient species observed after protonation of ${}^3\mathbf{1}$ in dilute aqueous acid is the conjugate acid ${}^3\mathbf{1H}^+$. The analysis of their data should be revised accordingly. In particular, the acidity constant is 2 orders of magnitude lower than previously estimated,⁵ $\text{p}K_{\text{a}}({}^3\mathbf{1H}^+) = -0.4 \pm 0.1$.

Conclusion

Rapid water addition to the triplet state of protonated benzophenone (${}^3\mathbf{1H}^+$) is responsible for the hitherto unexplained quenching of aromatic ketone triplets by protons in water. The rate constant for protonation of ${}^3\mathbf{1}$ is well below the diffusion-controlled limit, and this is attributed to a state symmetry-imposed barrier for adiabatic proton transfer to ${}^3\mathbf{1}$ (n,π^*) yielding ${}^3\mathbf{1H}^+$ (π,π^*). The acidity constant of ${}^3\mathbf{1H}^+$ is revised to $\text{p}K_{\text{a}}({}^3\mathbf{1H}^+) = -0.4 \pm 0.1$. Up to $[\text{H}^+] \leq 1$ M, protonation of ${}^3\mathbf{1}$ is rate-limiting for adiabatic hydration of ${}^3\mathbf{1H}^+$, which yields predominantly the *meta*-hydrate ${}^3\mathbf{1}\cdot\text{H}_2\text{O}$. The photohydration

reaction is reversible for parent **1** and **2**. Derivatives of **1** and **2** carrying fluoride as a leaving group in the meta position form the corresponding *m*-hydroxy derivatives cleanly and efficiently, constituting a hitherto unexplored, efficient aromatic photosubstitution reaction.

Acknowledgment. This work was supported by the Swiss National Science Foundation, Project Nos. 20-61746.00 and 2160-064525.01/1. We thank Sonja Mayer for skillful experimental support.

Supporting Information Available: HNMR of benzophenone in irradiated solution. This material is available free of charge via the Internet at <http://pubs.acs.org>.

References and Notes

- (1) Moore, W. M.; Hammond, G. S.; Foss, R. P. *J. Am. Chem. Soc.* **1961**, *83*, 2789–2794.
- (2) Tolbert, L. M.; Solntsev, K. M. *Acc. Chem. Res.* **2002**, *35*, 19–27.
- (3) Ledger, M. B.; Porter, G. *J. Chem. Soc., Faraday Trans. 1* **1972**, *68*, 539–553.
- (4) Ireland, J. F.; Wyatt, P. A. H. *J. Chem. Soc., Faraday Trans. 1* **1973**, *69*, 161–168.
- (5) Rayner, D. M.; Wyatt, P. A. H. *J. Chem. Soc., Faraday Trans. 2* **1974**, *70*, 945–954.
- (6) Favaro, G.; Bufalini, G. *J. Phys. Chem.* **1976**, *80*, 800–804.
- (7) Rayner, D. M.; Tolg, P. K.; Szabo, A. G. *J. Phys. Chem.* **1978**, *82*, 86–89.
- (8) Shizuka, H.; Kimura, E. *Can. J. Chem.* **1984**, *62*, 2041–2046.
- (9) Bensasson, R. V.; Gramain, J.-C. *J. Chem. Soc., Faraday I* **1980**, *76*, 1801–1810.
- (10) Lougnot, D. J.; Jacques, P.; Fouassier, J. P.; Casal, H. L. Kim-Thuan, N.; Scaiano, J. C. *Can. J. Chem.* **1985**, *63*, 3001–3006.
- (11) Hoshi, M.; Shizuka, H. *Bull. Chem. Soc. Jpn.* **1986**, *59*, 2711–2715.
- (12) Elisei, F.; Favaro, G.; Görner, H. *J. Photochem. Photobiol. A: Chem.* **1991**, *59*, 243–253.
- (13) Canonica, S.; Hellrung, B.; Wirz, J. *J. Phys. Chem. A* **2000**, *104*, 1226–1232.
- (14) Hasler, E.; Hörmann, A.; Persy, G.; Platsch, H.; Wirz, J. *J. Am. Chem. Soc.* **1993**, *115*, 5400–5409.
- (15) Senn, P.; Wirz, J. *Res. Chem. Intermed.* **1995**, *21*, 877–883.
- (16) Ni, T.; Caldwell, R. A.; Melton, L. A. *J. Am. Chem. Soc.* **1989**, *111*, 457–464. (b) Melton, L. A.; Ni, T.; Lu, Q. *Rev. Sci. Instrum.* **1989**, *60*, 3217–3223. (c) Arnaut, L. G.; Caldwell, R. A.; Elbert, J. E.; Melton, L. A. *Rev. Sci. Instrum.* **1992**, *63*, 5381–5389.
- (17) Gauglitz, G.; Hubig, S. *J. Photochem.* **1985**, *30*, 121–125.
- (18) Kresge, A. J.; Chen, H. J.; Capen, G. L.; Powell, M. F. *Can. J. Chem.* **1983**, *61*, 249–256.
- (19) The quoted delays relative to the subpicosecond excitation pulse refer to the blue end of the spectrum (300 nm). Red-shifted colors of the probe continuum reach the sample with smaller delays (chirping, ca. –1 ps delay per 80 nm shift), i.e., a quoted delay of 5 ps corresponds to a delay of 1.5 ps at 600 nm. Colors arriving simultaneously with the pump pulse are depleted by two photon absorption.
- (20) Arguments for the assignment of transient intermediates are given in the Discussion.
- (21) Gampp, H.; Maeder, M.; Meyer, C. J.; Zuberbühler, A. D. *Talanta* **1985**, *32*, 95–101.
- (22) Buxton, G. V.; Helman, W. P.; Ross, A. B. *J. Phys. Chem. Ref. Data* **1988**, *17*, 513–886.
- (23) Jonah, C. D.; Miller, J. R.; Matheson, M. S. *J. Phys. Chem.* **1977**, *81*, 931–934.
- (24) Frisch, M. J.; Trucks, G. W.; Schlegel, H. B.; Scuseria, G. E.; Robb, M. A.; Cheeseman, J. R.; Zakrzewski, V. G.; Montgomery, J. A., Jr.; Stratmann, R. E.; Burant, J. C.; Dapprich, S.; Millam, J. M.; Daniels, A. D.; Kudin, K. N.; Strain, M. C.; Farkas, O.; Tomasi, J.; Barone, V.; Cossi, M.; Cammi, R.; Mennucci, B.; Pomelli, C.; Adamo, C.; Clifford, S.; Ochterski, J.; Petersson, G. A.; Ayala, P. Y.; Cui, Q.; Morokuma, K.; Malick, D. K.; Rabuck, A. D.; Raghavachari, K.; Foresman, J. B.; Cioslowski, J.; Ortiz, J. V.; Stefanov, B. B.; Liu, G.; Liashenko, A.; Piskorz, P.; Komaromi, I.; Gomperts, R.; Martin, R. L.; Fox, D. J.; Keith, T.; Al-Laham, M. A.; Peng, C. Y.; Nanayakkara, A.; Gonzalez, C.; Challacombe, M.; Gill, P. M. W.; Johnson, B. G.; Chen, W.; Wong, M. W.; Andres, J. L.; Head-Gordon, M.; Replogle, E. S.; Pople, J. A. *Gaussian 98*; Gaussian, Inc.: Pittsburgh, PA, 1998.
- (25) Murov, S. L.; Carmichael, I.; Hug, G. L. *Handbook of Photochemistry*, 2nd ed.; Dekker: New York, 1993.
- (26) Carmichael, I.; Hug, G. L. *J. Phys. Chem. Ref. Data* **1986**, *15*, 1–250.
- (27) Assuming a molar absorption coefficient ϵ of ca. 30 000 M⁻¹ cm⁻¹, we estimate a quantum yield of <10% for the formation of *o*-1•H₂O in aqueous acid.
- (28) Miyasaka, H.; Morita, K.; Kamada, K.; Mataga, N. *Bull. Chem. Soc. Jpn.* **1990**, *63*, 3385–3397.
- (29) Tamai, N.; Asahi, T.; Masuhara, H. *Chem. Phys. Lett.* **1992**, *198*, 413–418.
- (30) Pelliccioli, A.-P.; Klán, P.; Zabadal, M.; Wirz, J. *J. Am. Chem. Soc.* **2001**, *123*, 7931–7932.
- (31) Godfrey, T. S.; Hilpern, J. W.; Porter, G. *Chem. Phys. Lett.* **1967**, *1*, 490–492.
- (32) Elmer, F.-J. *Differentialgleichungen in der Physik*; Verlag Harri Deutsch: Frankfurt am Main, 1997. (b) Mauser, H.; Gauglitz, G. Photochemistry, Theoretical Fundamentals and Applications; In *Chemical Kinetics*; Compton, R. G., Hancock, G., Eds.; Elsevier: Amsterdam, 1998; Vol. 36.
- (33) Shizuka, H. *Acc. Chem. Res.* **1985**, *18*, 141–147.
- (34) Boyd, D. R.; McMordie, R. A. S.; Sharma, N. D.; More O'Ferrall, R. A.; Kelly, S. C. *J. Am. Chem. Soc.* **1990**, *112*, 7822–7823. (b) Rao, S. N.; More O'Ferrall, R. A.; Kelly, S. C.; Boyd, D. R.; Agarwal, R. J. *Am. Chem. Soc.* **1993**, *115*, 5458–5465. (c) Dey, J.; O'Donoghue, A. C.; More O'Ferrall, R. A. *J. Am. Chem. Soc.* **2002**, *124*, 8561–8574.
- (35) Eigen, M. *Angew. Chem.* **1963**, *75*, 489–508.
- (36) Bagno, A.; Lucchini, V.; Scorrano, G. *J. Phys. Chem.* **1991**, *95*, 345–352.
- (37) The case for energy transfer to biacetyl from the short-lived species in the data of Favaro and Bufalini is weak. We were unable to observe energy transfer from ³H⁺ by transient absorption.
- (38) Favaro, G. *Chem. Phys. Lett.* **1975**, *31*, 87–90. (b) Favaro, G.; Romani, A. *Chem. Phys. Lett.* **1991**, *184*, 596–598.